



Transport of sulfadiazine in soil columns — Experiments and modelling approaches

Anne Wehrhan ^{a,*}, Roy Kasteel ^a, Jirka Simunek ^b, Joost Groeneweg ^a,
Harry Vereecken ^a

^a *Agrosphere, ICG IV, Forschungszentrum Jülich GmbH, Leo-Brandt Str., 52425 Jülich, Germany*

^b *Department of Environmental Sciences, University of California, Riverside, CA, 92521, USA*

Received 2 November 2005; received in revised form 14 July 2006; accepted 13 August 2006

Available online 6 October 2006

Abstract

Antibiotics, such as sulfadiazine, reach agricultural soils directly through manure of grazing livestock or indirectly through the spreading of manure or sewage sludge on the field. Knowledge about the fate of antibiotics in soils is crucial for assessing the environmental risk of these compounds, including possible transport to the groundwater. Transport of ¹⁴C-labelled sulfadiazine was investigated in disturbed soil columns at a constant flow rate of 0.26 cm h⁻¹ near saturation. Sulfadiazine was applied in different concentrations for either a short or a long pulse duration. Breakthrough curves of sulfadiazine and the non-reactive tracer chloride were measured. At the end of the leaching period the soil concentration profiles were determined. The peak maxima of the breakthrough curves were delayed by a factor of 2 to 5 compared to chloride and the decreasing limbs are characterized by an extended tailing. However, the maximum relative concentrations differed as well as the eluted mass fractions, ranging from 18 to 83% after 500 h of leaching. To identify relevant sorption processes, breakthrough curves of sulfadiazine were fitted with a convective–dispersive transport model, considering different sorption concepts with one, two and three sorption sites. Breakthrough curves can be fitted best with a three-site sorption model, which includes two reversible kinetic and one irreversible sorption site. However, the simulated soil concentration profiles did not match the observations for all of the used models. Despite this incomplete process description, the obtained results have implications for the transport behavior of sulfadiazine in the field. Its leaching may be enhanced if it is frequently applied at higher concentrations.

© 2006 Elsevier B.V. All rights reserved.

Keywords: Sulfadiazine transport; Antibiotics; Soil column; Breakthrough curve; Transport models; Sorption models

* Corresponding author. Now working at: Federal Environment Agency, postbox 1406, 8 06813 Dessau, Germany. Tel.: +49 340 2103 3151; fax: +49 340 2104 3151.

E-mail address: anne.wehrhan@uba.de (A. Wehrhan).

1. Introduction

Among other veterinary pharmaceuticals sulfadiazine (SDZ), which belongs to the group of sulfonamides, is a widely used antimicrobial substance in intensive livestock production to treat and prevent diseases (Thiele-Bruhn, 2003; Boxall et al., 2004). Up to 40% of the administered sulfonamides are eliminated as microbial active parent substances with the animal excretions (Kroger, 1983). Manure is dropped directly onto the pastures by grazing livestock or spread onto agricultural soils after storage as fertilizer (Jørgensen and Halling-Sørensen, 2000). Concentrations of SDZ measured in pig manure range between 0.3 and 198 mg of SDZ per kg depending on medication, dilution and age of the manure (Höper et al., 2002; Grote et al., 2004; Hamscher et al., 2005). As a result of the wide distribution of manure in the environment, sulfonamides are frequently found at concentration levels between a few and 100 ng L⁻¹ in surface waters of Northwestern Germany (Christian et al., 2003). Due to low extraction efficiencies (Kreuzig et al., 2003; Hamscher et al., 2005), there are no reliable data for typical SDZ concentrations in soils. The risk of surface water contamination is enhanced by surface runoff from manured fields (Burkhardt et al., 2005; Kay et al., 2005a) or in drained arable lands. Peak concentrations of about 0.6 mg L⁻¹ of sulfachloropyridazine and 0.03 mg L⁻¹ of oxytetracycline, two other antibiotic substances used in pig breeding, were found in drainage water after the application of contaminated pig manure (Kay et al., 2004).

During monitoring of pharmaceuticals in groundwater in southwest Germany, SDZ was found in one out of 105 samples (Sacher et al., 2001). In contrast to another sulfonamide (sulfamethazine) or tetracyclines, SDZ was not detected in the soil or groundwater after the application of contaminated pig manure to a field site (Hamscher et al., 2005). Possible reasons for the fast dissipation of SDZ compared to the other substances are either a faster degradation or transformation, strong sorption in non-extractable fractions or low extraction efficiencies of soil analysis (Hamscher et al., 2005). It is known that the recovery of SDZ from spiked soil samples decreases with time from 74% to 18% for samples extracted 5 min or 7 days after spiking (Hamscher et al., 2005). The contact times of the antibiotics and the soil matrix are typically far longer in the field, provided that very fast degradation can be excluded.

Mineralization of ¹⁴C-labelled SDZ to ¹⁴CO₂ in bovine manure, soil or soil manure slurries is less than 2% after 102 days (Kreuzig and Höltge, 2005), which we also found in separate investigations with the same soil without manure (data not shown). However, Kreuzig and Höltge (2005) found that the dissipation of SDZ in the extracts was much faster (after one week only 40, 20 or 5% of the initially applied ¹⁴C was detectable in manure, soil or soil manure slurries, respectively). They attributed this to the fixation of SDZ or its transformation products as non-extractable residues. They also detected up to four unidentified transformation products by radio thin layer chromatography in the remaining extractable fraction. This study was in contrast to another investigation, where no substances other than SDZ were found in comparable extracts (Kreuzig et al., 2003).

Looking into the pharmacokinetics, one of these metabolites might be acetyl-SDZ. Within treated pigs, SDZ is metabolized to the N4-acetyl-sulfadiazine and both substances are mainly eliminated by renal excretion (Kroger, 1983; Grote et al., 2004) and thus found in manure. However, de-acylation leads to an increasing concentration of SDZ in stored manure (Berger et al., 1986; Grote et al., 2004). Although those studies focused on the metabolism in manure, the results of Kreuzig and Höltge (2005) and our separate experiments (unpublished data) indicate

that transformation reactions might also occur in soils. Additional to acetyl-SDZ, Pfeifer et al. (2005) detected hydroxy-SDZ in pig manure. In contrast to acetyl-SDZ, hydroxy-SDZ can still be active against different bacteria strains. It is therefore essential to investigate the fate of both, the parent and possible transformation products.

To prevent further environmental contamination and possible adverse effects of the antimicrobial substances on soil microbial populations, an understanding of the environmental fate of these compounds is necessary (Jørgensen and Halling-Sørensen, 2000). Apart from the route of entry, the fate of pharmaceuticals in the environment is comparable to other organic chemicals, such as pesticides. The literature on sorption and transport of organic chemicals in soils is for instance compiled in the review articles by Pignatello and Xing (1996) and Flury (1996). To assess the mobility of pollutants in the environment, knowledge about their persistence and sorption behavior is crucial. Until now the sorption/desorption processes of SDZ in soils are not thoroughly investigated. Sorption studies with sulfadiazine and other sulfonamides and different soils showed a Freundlich-type behavior with typical equilibrium times of 16 h (Thiele-Bruhn and Aust, 2003). Formation of non-extractable residues of ^{14}C -labelled SDZ was observed in a clayey silt (Kreuzig et al., 2003). Whereas about 50% of SDZ was not extractable after three days of incubation in this study, this fraction increased to about 90% after 28 days. Therefore, concentration- and time-dependent and possibly also irreversible sorption can be expected in soils.

Process-oriented studies are scarce in literature concerning the transport of SDZ in soils. The mobility of sulfonamides in soils is assumed to be high, based on their physicochemical properties (Tolls, 2001). However, incomplete breakthrough of SDZ was observed in several transport studies. SDZ was rarely found in the leachate of column and plot studies, and most of the applied SDZ was retained in the upper part of the soil (Kreuzig and Höltege, 2005). Fast sorption of SDZ into non-extractable pools was reported in leaching experiments with undisturbed soil columns, after application of contaminated manure (Kreuzig and Höltege, 2005). Sulfachloropyridazine, which is a sulfonamide similar to SDZ, was found to be quite mobile, but also readily degradable (Boxall et al., 2002; Kay et al., 2004, 2005a,b). The component was classified as being mobile in different soils from two-days batch sorption experiments, which was additionally verified in column studies (Boxall et al., 2002). However, the leached mass fraction was lower than expected, and the non-recovered mass in the experiments was attributed to degradation (Boxall et al., 2002; Kay et al., 2005b). Similar observations were also reported for sulfamethoxazole: leaching was shown to depend on (i) the applied mass, (ii) irrigation intensity and (iii) soil type (Drillia et al., 2005), which hints towards a soil dependent, non-linear and time-dependent sorption of the investigated sulfonamide.

To our knowledge transport and sorption mechanisms of sulfadiazine have not yet been systematically analyzed in column experiments. The objective of this study was to investigate the transport behavior of sulfadiazine in disturbed soil columns at a constant flow rate near saturation. We especially focus on the effect of concentration on the fate of SDZ, by changing the input concentration and/or pulse duration. Although the antibiotics enter the soil environment typically as ingredients of manure, the experiments were performed without manure to circumvent any changes in soil properties (e.g. pH, ionic strength, dissolved and particulate organic matter) and their effects on solute transport. ^{14}C -labelled SDZ was used to ensure complete mass balances. To identify relevant sorption processes, measured breakthrough curves (BTCs) and soil concentration profiles of SDZ were fitted with a convective–dispersive transport model considering different sorption concepts.

2. Theory of solute transport

The transport of non-degradable dissolved substances in homogeneous soils with a constant water content and steady state flow conditions is typically described by the convection–dispersion equation (CDE) (e.g. Hillel, 1998):

$$\frac{\partial C_t}{\partial t} = D\theta \frac{\partial^2 C}{\partial z^2} - j_w \frac{\partial C}{\partial z} \quad , \quad (1)$$

where t is time [T], z is depth [L], D is the hydrodynamic dispersion coefficient [$L^2 T^{-1}$], θ is the volumetric water content [$L^3 L^{-3}$], j_w is the water flow density [$L T^{-1}$], C is the solute concentration in the liquid phase [$M L^{-3}$] and C_t is the total mass of solute per unit volume of soil [$M L^{-3}$]. For non-volatile compounds C_t is given as the sum of concentrations in the dissolved and sorbed phase:

$$C_t = \theta C + \rho S \quad , \quad (2)$$

where ρ is the soil bulk density [$M L^{-3}$] and S is the sorbed solute concentration [$M M^{-1}$].

2.1. Sorption models

Various sorption concepts are available to describe the interaction of dissolved substances with the soil material. These sorption concepts differ with respect to the involved sorption isotherm (linear or non-linear), the assumptions made concerning the time-dependency (instantaneous or rate-limited) and reversibility of the sorption process (reversible or irreversible). Up to three sorption regions were considered in our study. Multiple sorption regions are considered in sorption models to represent the heterogeneity of the soil material with respect to its sorption properties as well as differences in the accessibility of the potentially sorptive surfaces. However, these sorption regions are only conceptual and do not reflect well-defined fractions of the soil material. We compare the isotherm-based distribution models to the attachment/detachment approach. Whereas the former approach describes the equilibrium distribution between phases by an adsorption isotherm, the latter is based on multiple kinetic processes. It was introduced to describe the transport of small particles or bacteria through porous media (e.g. Schijven and Hassanizadeh, 2000; Bradford et al., 2003). The solute–soil–water distribution models considered in this study are summarized in Fig. 1.

2.2. Isotherm-based models

A comprehensive mathematical derivation of the applied sorption models is given elsewhere in detail (e.g. Streck et al., 1995). Therefore, we give here only their implementation into the solute transport equation. The combination of Eqs. (1) and (2) results in:

$$\theta \frac{\partial C}{\partial t} + \rho \frac{\partial S}{\partial t} = \theta D \frac{\partial^2 C}{\partial z^2} - j_w \frac{\partial C}{\partial z} \quad . \quad (3)$$

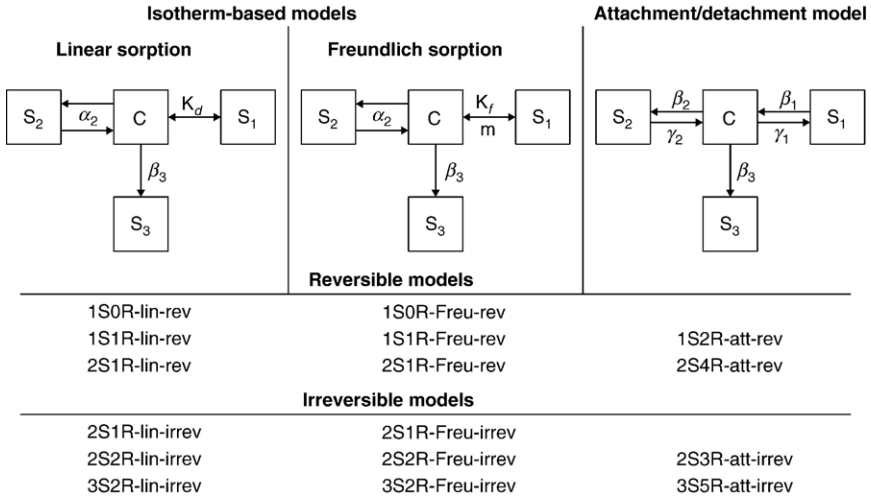


Fig. 1. Structures of the applied models. The boxes labelled with C represent the liquid phase with concentration C , the boxes S_i , with $i=1,2,3$ represent the three sorption sites with the respective concentrations. The arrows indicate the sorption process, where K_d is the distribution coefficient, K_f and m are the Freundlich coefficient and exponent, $\hat{\alpha}_2$ is the reversible ad- and desorption rate, β_i and γ_i are the one-way attachment and detachment rates, respectively. Simplified versions of each model were derived by omitting one or two sorption sites: The combinations for reversible and irreversible models are given below the models. The model names are composed of the number of sites, S (1–3), number of rates, R (0–5), sorption concept (lin: linear and Freu: Freundlich sorption isotherms, att: attachment/detachment model) and reversibility of the sorption process (rev: reversible, irrev: irreversible).

2.2.1. One-site equilibrium sorption

For instantaneously and reversibly sorbing substances Eq. (3) can be rewritten as:

$$R \frac{\partial C}{\partial t} = D \frac{\partial^2 C}{\partial z^2} - v \frac{\partial C}{\partial z}, \tag{4}$$

where $v=j_w/\theta$ is the pore water velocity [$L T^{-1}$] and R [-] is the retardation factor:

$$R = 1 + \frac{\rho}{\theta} \frac{\partial S}{\partial C}, \tag{5}$$

where $\partial S/\partial C$ is the first derivative of a relationship between the concentration in the solid (S) and liquid (C) phases, expressed by the sorption isotherm. The linear and non-linear (Freundlich) isotherms are given by:

$$S = K_d C, \tag{6}$$

where K_d is the soil–water distribution coefficient [$L^3 M^{-1}$] and:

$$S = K_f C^m, \tag{7}$$

where K_f is the Freundlich distribution coefficient [$M_{solute}^{1-m} L^{3m} M_{soil}^{-1}$] and m is the dimensionless Freundlich exponent. Note that the linear isotherm is a special case of the Freundlich isotherm for $m=1$. The retardation factor R is given by:

$$R = 1 + \frac{\rho}{\theta} K_f m C^{m-1}. \tag{8}$$

The 1S0R-lin-rev and 1S0R-Freu-rev models (Fig. 1) are given by Eqs. (4) and (8).

2.2.2. One-site, rate-limited, reversible sorption

If the equilibrium distribution of the solute between solid and liquid phases cannot be considered instantaneous, a kinetic term may be introduced (Fortin et al., 1997):

$$\frac{dS}{dt} = \alpha(K_f C^m - S) \quad , \quad (9)$$

where α is the adsorption/desorption rate coefficient [T^{-1}]. The combination of Eqs. (3) and (9) (van Genuchten and Wierenga, 1976) yields the 1S1R-lin-rev and 1S1R-Freu-rev models (Fig. 1, the subscript 2 is dropped in the equation for simplicity in the one-site model).

2.2.3. Two-site, rate-limited, reversible sorption

Two-site sorption to instantaneous (S_1) and rate-limited sorption sites (S_2) is described by the following set of equations (van Genuchten and Wagenet, 1989; Simunek et al., 1998):

$$S = S_1 + S_2 \quad , \quad (10)$$

$$S_1 = f K_f C^m \quad , \quad (11)$$

$$\frac{dS_2}{dt} = \alpha_2((1-f)K_f C^m - S_2) \quad , \quad (12)$$

where f is the fraction of equilibrium sites (S_1), and α_2 is the sorption rate coefficient [T^{-1}]. Together with Eq. (3) it gives the 2S1R-lin-rev and 2S1R-Freu-rev models (Fig. 1).

2.2.4. Irreversible sorption

Irreversible sorption is represented as a first-order kinetic sink of solute in the water phase. This process is equivalent to the description of the first-order degradation from the water phase (Prata et al., 2003) and is given by Eq. (13), assuming that sorption sites S_3 exhibit irreversible sorption:

$$\frac{\partial S_3}{\partial t} = -\frac{\theta}{\rho} \beta_3 C \quad , \quad (13)$$

where β_3 is the irreversible adsorption rate coefficient [T^{-1}]. In the three-sites two-rates irreversible sorption models (3S2R-lin-irrev and 3S2R-Freu-irrev) total sorbed concentration S is then given by:

$$S = S_1 + S_2 + S_3 \quad , \quad (14)$$

where sorption characteristics for S_1 and S_2 are described by Eqs. (11) and (12), respectively. In the 2S2R-lin-irrev and 2S2R-Freu-irrev models the instantaneous sorption sites S_1 are omitted ($f=0$), whereas the rate-limited reversible sorption sites S_2 are omitted ($f=1$) in the 2S1R-lin-irrev and 2S1R-Freu-irrev models.

2.3. Attachment/detachment models

In the attachment/detachment concept all processes are first-order and rate-limited. Reversible attachment/detachment processes are given by:

$$\frac{\partial S_i}{\partial t} = \frac{\theta}{\rho} \beta_i C - \gamma_i S_i \quad , i = 1, 2 \quad , \quad (15)$$

where β_i are the attachment and γ_i the detachment rate coefficients [T^{-1}] for the corresponding attachment/detachment sites S_i . If detachment is omitted, the second term on the right hand side of Eq. (15) goes to zero. Thus, Eq. (15) is equivalent to Eq. (13), i.e. it describes irreversible sorption. Equally to the isotherm-based models the total sorbed concentration is given by Eq. (14). The attachment/detachment model with two reversible and one irreversible site (3S5R-att-irrev) is given by the combination of Eqs. (3, 13–15) (Schijven and Šimuňek, 2002). Simpler attachment/detachment models with less sites or rates are derived by setting selected rate parameters to zero: $\beta_3=0$ in the 2S4R-att-irrev model, $\gamma_2=\beta_2=0$ in the 2S3R-att-irrev model and $\beta_3=\gamma_2=\beta_2=0$ in the 1S2R-att-irrev model.

2.3.1. Comparison of isotherm-based and attachment/detachment concept

In the attachment/detachment concept the ratio of the first-order attachment and detachment rate coefficients describes the tendency of the solute to distribute in either the liquid or the solid phase. This eventually results in linear equilibrium distribution isotherms, such as the isotherm-based models with linear sorption. However, the concept of the isotherm-based and the attachment/detachment model differs in whether the interaction occurs to the bulk soil or to only one fraction (f , $(1-f)$) of the bulk soil. Whereas the sorption parameters of the isotherm-based modes are independent of the experimental conditions, the attachment/detachment model parameters depend on θ and ρ and are therefore not readily comparable between varying soil to solution ratios. Despite the difference in mathematical formulation, the attachment/detachment model can be parameterized in such a way, that it is equivalent to the linear sorption model with a similar number of rate-limited sorption sites (e.g. 1S1R-lin-irrev equals 1S2R-att-irrev, and 2S2R-lin-irrev equals 2S3R-att-irrev). If the attachment and detachment rates in one sorption site are much faster compared to the other processes, it can be described as instantaneous. In this case the models 2S1R-lin-irrev and 2S4R-att-irrev as well as 3S2R-lin-irrev and 3S5R-att-irrev are equivalent, too. However, the 3S5R-att-irrev model is more flexible than the 3S2R-lin-irrev model because it considers all sorption processes to be rate-limited.

3. Materials and methods

All transport experiments were done with the antimicrobial substance sulfadiazine (IUPAC-name: 4-amino-*N*-pyrimidin-2-yl-benzenesulfonamide, Fig. 2). Selected physicochemical properties are listed in Table 1. The transport studies were conducted in repacked soil columns near water saturation. Three experiments with different input scenarios (A, B, C) were performed in order to investigate the effect of concentration and pulse duration on the fate of SDZ (Table 2). Whereas in experiments A and B solute was applied for a long pulse duration, solute was applied with a short pulse in experiment C. High solute concentrations were applied in experiments A and C. Only about one tenth of that concentration was applied in experiment B. Thus, the total applied solute masses were approximately equal for experiments B and C.

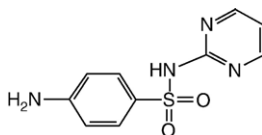


Fig. 2. Chemical structure of sulfadiazine (SDZ). The ^{14}C -labelling is in the phenyl-ring with a specific radioactivity of 3.46 MBq mg^{-1} .

3.1. Soil columns

The soil material was collected from the upper 30 cm of an Eutric Cambisol which was used as grassland in the past. The soil is classified as a silty loam and characterized as described in Table 3. Field moist soil was sieved (2 mm) and stored at 4°C in the dark until usage.

The columns were made of stainless steel (inner diameter and height were 8.5 cm and 10 cm, respectively). They were mounted on a porous ceramic plate (high flow, air-entry point >1 bar). The outflow was connected to a fraction collector. An irrigation device with 12 glass needles was placed on top of the column. An HPLC-pump (high performance liquid chromatography) supplied a constant irrigation from a reservoir. No pressure was applied at the bottom of the soil column.

Wet soil (gravimetric water content of 40%) was packed in the columns in small increments, each compacted with a metal stick, up to a total height of 9 cm. Due to the sticky properties of the fine textured soil, the wet soil could not be compacted to a typical field soil bulk density. A density of about 1 g cm^{-3} (Table 4) assured the maintenance of constant flow rates. A 0.5 cm thick layer of coarse quartz sand was put on top of the packed soil in order to provide a more uniform distribution of water and to prevent splashing of the soil material. This sand was burnt in an oven at 450°C for 24 h to remove any organic contamination. The soil columns were saturated from the bottom with a 0.01 M CaCl_2 solution for three days.

3.2. Transport experiments

The soil columns were irrigated at a constant rate of approximately 0.26 cm h^{-1} for four days to establish steady state flow conditions. The pistons of the pump were flushed with water once a day to prevent salt precipitation and drying. Although the flow rate was regulated by the HPLC-

Table 1
Selected physicochemical properties of sulfadiazine

Molecular formula		$\text{C}_{10}\text{H}_{10}\text{N}_4\text{O}_2\text{S}$
CAS [†]		68-35-9
Molecular mass	[g mol ⁻¹]	250.28
pK _{a1} and pK _{a2} [‡]		1.57 and 6.50
Melting point	[°C]	250
Vapor pressure	[Pa]	5.745×10^{-6}
Henry constant	[Pa m ³ mol ⁻¹]	1.60×10^{-5}
Solubility in water	[mg L ⁻¹]	13 to 77
Octanol/water distribution coefficient		0.76
Specific radioactivity [§]	[MBq mg ⁻¹]	3.46

Data were taken from the supplier of the non-labelled SDZ: Sigma Aldrich, Taufkirchen, Germany. [†]Registration number of the Chemical Abstract Service; [‡]acidity constants; [§]for the labelled compound supplied by the Institute of Isotopes Co., Ltd., Budapest, Hungary.

Table 2
Experimental conditions of the column experiments

Soil column	C_0^\dagger (mg L ⁻¹)	V_{in}^\ddagger (L)	Δt_{in}^\S (h)	m_{in}^\P (mg)	$M_{app}^\#$ (g m ⁻²)	$j_w^{\dagger\dagger}$ (cm h ⁻¹)
A	5.70	1.047	67.8	5.97	1.052	0.266
B	0.57	1.032	68.0	0.526	0.093	0.260
C	5.70	0.094	7.0	0.539	0.095	0.262

[†]SDZ concentration in the application solution, [‡]volume of application solution, [§]pulse duration, [¶]applied mass, [#]applied mass per soil surface area, ^{††}irrigation rate.

pump, it was additionally controlled by weighing the solution loss from the reservoir per unit time as well as the leached volume in the single fractions.

A defined volume of the application solution of chloride or SDZ was irrigated on top of the column and subsequently leached with the 0.01 M CaCl₂ solution at the same flow rate. The applied volume was determined by the mass difference in the reservoir.

Measured concentrations in single fractions of the leachate were corrected for evaporation losses (approximately 4.5×10^{-6} L h⁻¹) during the open sample storage in the fraction collector. For a better comparison between the experiments, concentrations in the outflow were normalized to their corresponding input concentrations (C_0).

3.2.1. Chloride

A breakthrough curve of chloride as a non-reactive tracer was determined for each packed soil column to characterize the flow behavior of water itself. The chloride was applied as a 2-h pulse

Table 3
Some selected physical and chemical properties of the soil material

Parameter	Unit	Value
Texture [†] :		
Clay (<0.002 mm)	[% mass] [‡]	23
Fine silt (0.002–0.006 mm)	[% mass]	7
Medium silt (0.006–0.020 mm)	[% mass]	14
Coarse silt (0.020–0.063 mm)	[% mass]	22
Fine sand (0.063–0.200 mm)	[% mass]	19
Medium sand (0.200–0.630 mm)	[% mass]	11
Coarse sand (0.630–2.000 mm)	[% mass]	4
Clay minerals [§] :		
Smectite	[%]	25
Illite	[%]	25
Chlorite	[%]	50
Specific surface area	[m ² g ⁻¹]	4.96
Chemical analysis [†] :		
pH		6.1
P_{tot}^\P	[mg kg ⁻¹]	1292
CEC [#]	[meq 100 g ⁻¹]	17.4
$C_{org}^{\dagger\dagger}$	[% mass]	3.3
$CaCO_3^{\ddagger\dagger}$	[% mass]	<3

Soil was air dried and sieved to 2 mm prior to the analysis. [†]Analysis were done by standard procedures at the laboratory of the LUFA (Landwirtschaftliche Untersuchungs-und Forschungsanstalt) in Speyer, Germany. [‡]The mass fractions are based on the total mass of soil. [§]Clay minerals were analyzed by X-ray diffraction at the Institute of Soil Science and Soil Ecology at the University of Bonn, Germany. [¶]Total content of phosphorous, [#]cation exchange capacity, ^{††}content of organic carbon, ^{‡‡}content of carbonate.

Table 4
Properties of the soil columns and the experimental conditions

Soil column	j_w (cm h ⁻¹)	ρ (g cm ⁻³)	v (cm h ⁻¹)	θ (cm ³ cm ⁻³)	D (cm ² h ⁻¹)	λ (cm)	EF [†]
A	0.266	0.89	0.437	0.609	0.580	1.329	0.990
B	0.260	0.99	0.492	0.528	0.191	0.388	0.997
C	0.262	0.84	0.543	0.483	0.258	0.475	0.983

The irrigation rate, j_w , and the soil bulk density, ρ , were determined experimentally. The pore water velocity, v , and the dispersion coefficient, D , were fitted to the BTCs of chloride. The volumetric water content, θ , and the dispersivity, λ , were calculated.

[†]Modelling efficiency according to Loague and Green (1991): $EF = (\sum(O_i - O_{mean})^2 - \sum(O_i - P_i)^2) / (\sum(O_i - O_{mean})^2)$, where O_i and P_i are the observed and predicted values, respectively and O_{mean} is the arithmetic mean of the observed values.

with an input concentration $C_0(\text{Cl}^-)$ of 1.0 g L⁻¹ as CaCl₂. The leachate was collected in hourly fractions of approximately 15 mL for analysis until a constant background level was reached.

The chloride concentration in the leachate was determined by measuring the electrical conductivity. The electrical conductivity linearly correlates with the concentration of CaCl₂ within the concentration range of the samples. Solutions with known concentrations of CaCl₂ were used to determine the calibration curve.

3.2.2. Sulfadiazine

The application solution of SDZ was prepared in 0.01 M CaCl₂ solution by addition of the appropriate amount of stock solution (500 mg SDZ L⁻¹ dissolved in acetonitrile). For experiment A ¹⁴C-labelled SDZ and non-labelled SDZ were mixed (1:4, m:m) to reduce the consumption of the labelled compound. In experiments B and C the ¹⁴C-labelled SDZ was not diluted with non-labelled SDZ to ensure adequate sample concentrations for analysis. The SDZ input solution was applied using the same steady irrigation rate as for chloride experiments. After application SDZ was eluted for 500 h, which corresponds to approximately 20 pore volumes. Detailed information about the experimental conditions is listed in Table 2.

The concentration of SDZ in the outflow was determined by measuring its ¹⁴C-radioactivity. An aliquot of the sample was mixed with 10 mL of an appropriate scintillation cocktail and measured by liquid scintillation counting (LSC). The detection limit of the LSC-method is 0.25 Bq per sample. The measuring volume V of the sample was chosen according to its expected specific radioactivity, varying from 0.1 to 5 mL for high and low specific radioactivities, respectively. Each sample was measured in triplicate. All measured values were corrected for the background radiation measured in a blank sample. The corresponding specific radioactivity A_{spec} [T⁻¹ L⁻³] was calculated from the measured radioactivity A [T⁻¹].

The equivalent SDZ concentration of the sample was determined after division by the specific radioactivity of the applied SDZ, A_{spec} (SDZ) [T⁻¹ M⁻¹] (0.865 and 3.46 MBq mg⁻¹ for experiment A and experiments B and C, respectively), assuming that ¹⁴C-radioactivity is linearly related to SDZ. If any transformation products were present the resulting total SDZ concentrations are the sum of both, parent and transformation products, given in mass equivalents of SDZ (molecular mass = 250.28 g mol⁻¹).

At the end of each leaching experiment, the soil was sliced at 0.5 or 1 cm depth intervals to determine the concentration distribution of SDZ in the column. For all samples the water content was determined gravimetrically. Prior to analysis the dry soil samples were ground and homogeneously mixed. The SDZ concentration in soil was determined by measuring the ¹⁴C-

radioactivity after total combustion of the soil samples with the help of an oxidizer. Three replicates of 0.500 g of each soil sample were combusted at 900 °C. The evolving gas was washed into a scintillation cocktail. Here, $^{14}\text{CO}_2$ was trapped and subsequently measured by LSC. The ^{14}C -analysis in both solid and liquid phases was insensitive to matrix effects and did not require any extraction steps.

The performance of the method was checked in each measuring series. Blanks were run before and after the samples to check for background contamination and cross contamination during the measurement. The recovery of the method is defined as the ratio of measured radioactivities in a blank sample spiked with a known amount of ^{14}C prior to combustion to the radioactivity in a blank sample where ^{14}C was spiked to the scintillation cocktail after combustion. Measurement series with a recovery <92% were repeated.

The total concentration of SDZ in the soil [$M(\text{SDZ}) \text{ M}^{-1}(\text{soil})$] is calculated from the mass of the soil, the specific radioactivity of the applied SDZ $A_{\text{spec}}(\text{SDZ})$, and the measured radioactivity corrected for the corresponding recovery. As discussed for the liquid phase concentrations above, SDZ concentrations in the solid phase refer to the sum of both, the parent compound and its transformation products, given in mass equivalents of SDZ. Note that the soil concentration is the sum of the sorbed and dissolved solute per unit mass of soil.

3.3. Parameter estimation

Water flow and solute transport in the soil columns were treated as one-dimensional problems in mathematical simulations. The water content was assumed to be constant in space and time throughout the experiment. Any variations in water content were assumed to be negligible, because the columns were homogeneously packed, water-saturated at the bottom and irrigated with a constant rate at the top. The columns were assumed to be initially solute free (Cl^- or SDZ). A flux concentration boundary was assumed at the top and a zero concentration gradient at the bottom of the column.

3.3.1. Conservative tracer chloride

The transport parameters ν and D were determined by fitting the analytical solution of the CDE (Eq. (4) with $R=1$) with appropriate initial and boundary conditions to the observed BTC using the CXTFIT code (Toride et al., 1999). To account for variations in mass balance, the input concentration was also fitted. From D , ν and j_w the volumetric water content $\theta=j_w/\nu$ and the dispersivity $\lambda=D/\nu$ were calculated and used to fix the water flow for the transport simulations with the reactive tracer SDZ.

3.3.2. Reactive tracer SDZ

Since SDZ exhibits non-linear sorption and no analytical solution exists for such transport behavior, we used the numerical code *HYDRUS-1D* (Simunek et al., 1998) to describe the transport experiments. *HYDRUS-1D* is a finite element code that provides numerical solutions for various transport models described above. The Galerkin finite element method with a Crank–Nicholson time weighting scheme was used to solve the governing solute transport equations. *HYDRUS-1D* includes an inverse parameter optimization method based on the Levenberg–Marquardt algorithm. For the numerical calculations the soil profile was discretized into 101 evenly distributed nodes. The maximum time step was chosen small enough to assure a mass balance error smaller than 1%. The model was run with gravity driven flow, where the hydraulic conductivity at the prevailing water content was set equal to the irrigation rate j_w .

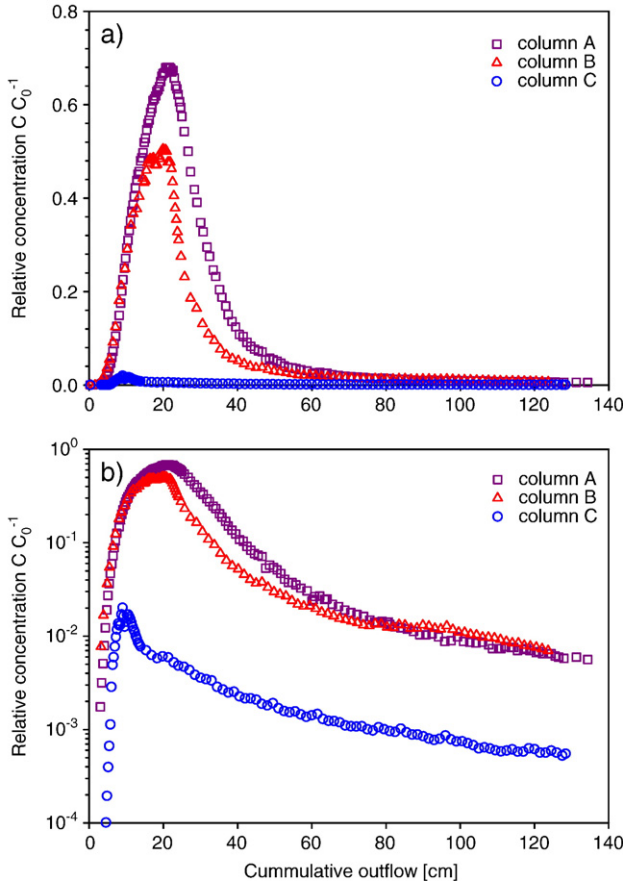


Fig. 3. Breakthrough curves of SDZ in the three columns plotted on a linear (a) and a logarithmic (b) scale.

HYDRUS-1D was used either in a predictive manner with fixed transport parameters or in an inverse mode to fit one or more parameters of a sorption model to the experimental data. In the latter case the experimental data of the BTC were in selected cases internally \log_{10} -transformed to increase the weighting on the BTC tailing. The soil concentration profile data were not transformed. Unit weights were assigned to all residuals. Either BTC, profile or both data sets were used in the fitting procedure. To evaluate the goodness of fit we calculated the modelling efficiency for the non-transformed (EF) and \log_{10} -transformed BTC data (EF_{\log}) according to [Loague and Green \(1991\)](#). A modelling efficiency equal to 1 indicates perfect agreement of the model and the data. If the modelling efficiency is negative, the arithmetic mean of the data is a better description for the data set than the model. The sum of squares was also calculated for the non-transformed (SSQ) and \log_{10} -transformed data (SSQ_{\log}). Due to different orders of magnitude of the concentration values in the peak and tailing of the BTC, a mismatch in the peak concentrations affects EF or SSQ more than deviations in the tailing. Deviations in the low concentration range (at the beginning and the end of the BTC) result in a larger SSQ_{\log} and a smaller EF_{\log} . Because transformation reactions can not be ruled out during our experiments, we focused on an effective transport description for the sum of SDZ and possible transformation

Table 5
Mass recovery of ^{14}C -radioactivity after the column experiments

Soil column	In leachate (% [†])	In soil column (%)	Total recovery (%)
A	82.7	14.5	97.2
B	60.7	38.3	99.0
C	17.8	81.8	99.6

[†]Mass fractions are given in percent of the applied mass, m_{in} (Table 2).

products. However, as the identity and fate of the possible transformation products are still unknown, the sum of SDZ and potentially active or re-transferable transformation products is of environmental concern. This lumped characterization can be used for a first risk assessment. This was previously done by Prata et al. (2003) and Casey et al. (2004), who also used ^{14}C -labelled compounds for their experiments. Despite the determination of transformation products in the leachate, they applied their models to the measured ^{14}C -data and the modelling resulted in an effective description of the transport behavior of the parent substance and its transformation products.

4. Results

4.1. Transport and breakthrough curves of chloride

The transport parameters D and ν that were fitted to the chloride BTCs are listed in Table 4. Although the obtained parameters were not identical for all three columns, the physical equilibrium CDE was able to describe all BTCs. It was, thus, concluded that no non-equilibrium processes affected the chloride transport and that there was no stagnant water. Relatively large differences in water contents between the three columns were likely due to the packing procedure that was difficult to standardize. To account for these variations in the flow field between columns, the transport parameters were individually determined for each column.

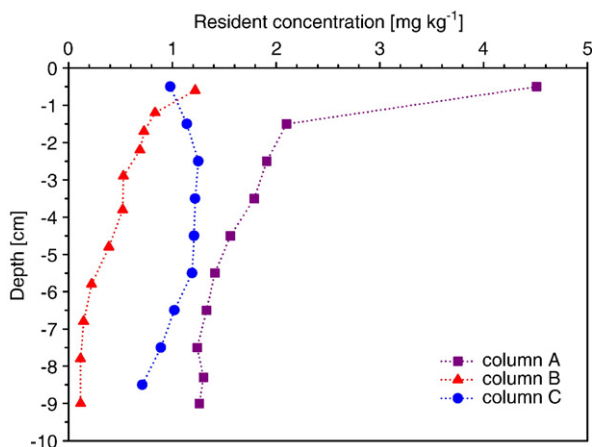


Fig. 4. Soil concentration profiles of resident ^{14}C concentrations in the three columns.

Table 6
Fitting parameters of the different isotherm-based (upper part) and attachment/detachment (lower part) models for column A

Model	Fit [†]	K_f ($\text{kg}^{-1}\text{L}^3\text{m}\text{mg}^{1-m}$)	m	α_2 (h^{-1})	f	β_3 (h^{-1})	EF [‡]	EF _{log} [§]	SSQ [¶]	SSQ _{log} ^{††}	EM ^{**} (%)
linear sorption models											
1S0R-lin-REV	Lin	$1.13 \times 10^{+0}$ ($8.77 \times 10^{+0}$)	1 [#]	0 [#]	1 [#]	0 [#]	0.864	-1.675	42.1	731	99
1S1R-lin-REV	Lin	$1.25 \times 10^{+0}$ (2.72×10^{-2})	1 [#]	8.67×10^{-2} (6.23×10^{-3})	0 [#]	0 [#]	0.956	0.407	13.7	162	99
2S1R-lin-REV	Lin	$4.39 \times 10^{+0}$ (2.67×10^{-1})	1 [#]	3.19×10^{-3} (2.72×10^{-4})	1.97×10^{-1} (1.16×10^{-2})	0 [#]	0.996	0.216	1.30	214	89
2S1R-lin-REV	Log	$1.54 \times 10^{+0}$ (2.20×10^{-2})	1 [#]	6.55×10^{-3} (2.80×10^{-4})	5.83×10^{-1} (8.13×10^{-3})	0 [#]	0.931	0.997	21.2	0.88	98
2S1R-lin-irREV	Lin	9.10×10^{-1} (1.02×10^{-2})	1 [#]	0 [#]	1 [#]	1.40×10^{-2} (3.33×10^{-4})	0.991	-3.576	2.80	1251	73
2S2R-lin-irREV	Lin	9.46×10^{-1} (9.85×10^{-3})	1 [#]	3.76×10^{-1} (4.20×10^{-2})	0 [#]	1.17×10^{-2} (3.56×10^{-4})	0.994	-1.715	1.89	742	77
3S2R-lin-irREV	Log	$1.61 \times 10^{+0}$ (4.65×10^{-2})	1 [#]	7.08×10^{-3} (1.44×10^{-3})	5.95×10^{-1} (1.84×10^{-2})	4.67×10^{-3} (3.56×10^{-4})	0.987	0.997	4.12	0.71	88
Freundlich sorption models											
1S0R-Freu-REV	Log	7.61×10^{-1} (1.65×10^{-1})	5.04×10^{-1} (1.65×10^{-1})	0 [#]	1 [#]	0 [#]	0.263	-0.547	228	423	99
1S1R-Freu-REV	Log	$2.48 \times 10^{+0}$ (4.86×10^{-2})	5.27×10^{-1} (4.96×10^{-3})	8.12×10^{-2} (1.81×10^{-3})	0 [#]	0 [#]	0.980	0.987	6.22	3.50	97
2S1R-Freu-REV	Lin	$4.55 \times 10^{+0}$ (2.68×10^{-1})	9.51×10^{-1} (1.55×10^{-2})	3.32×10^{-3} (2.78×10^{-4})	2.03×10^{-1} (1.16×10^{-2})	0 [#]	0.996	0.617	1.22	105	88

Model	Fit [†]	β_1 (h ⁻¹)	γ_1 (h ⁻¹)	β_2 (h ⁻¹)	γ_2 (h ⁻¹)	β_3 (h ⁻¹)	EF [‡]	EF _{log} [§]	SSQ [¶]	SSQ _{log} ^{††}	EM ^{‡‡} (%)
2S1R-Freu- <i>rev</i>	Log	$2.40 \times 10^{+0}$ (5.21×10^{-3})	3.34×10^{-1} (9.94×10^{-4})	1.09×10^{-1} (1.47×10^{-4})	1.72×10^{-3} (5.71×10^{-6})	0 [#]	0.837	0.554	50.6	122	95
2S1R-Freu- <i>irrev</i>	Lin	$1.05 \times 10^{+0}$ (3.55×10^{-2})	9.03×10^{-1} (2.10×10^{-2})	0 [#]	1 [#]	1.41×10^{-2} (3.13×10^{-4})	0.992	-0.232	2.55	337	73
2S2R-Freu- <i>irrev</i>	Log	$2.31 \times 10^{+0}$ (3.61×10^{-2})	4.89×10^{-1} (1.14×10^{-2})	7.78×10^{-2} (2.55×10^{-3})	0 [#]	8.96×10^{-3} (9.87×10^{-4})	0.975	0.995	7.43	1.28	80
3S2R-Freu- <i>irrev</i>	Log	$2.33 \times 10^{+0}$ (3.21×10^{-2})	4.88×10^{-1} (1.63×10^{-2})	7.35×10^{-2} (4.61×10^{-5})	3.63×10^{-3} (1.17×10^{-2})	1.02×10^{-2} (8.60×10^{-4})	0.966	0.995	10.64	1.35	78
Attachment/detachment models											
1S2R-att- <i>rev</i>	Lin	1.59×10^{-1} (1.10×10^{-2})	8.74×10^{-2} (6.47×10^{-3})	0 [#]	0 [#]	0 [#]	0.956	0.403	13.7	163	99
2S3R-att- <i>irrev</i>	Lin	5.44×10^{-1} (6.65×10^{-2})	3.94×10^{-1} (4.98×10^{-2})	0 [#]	0 [#]	1.18×10^{-2} (3.51×10^{-4})	0.994	-1.760	1.90	755	77
2S4R-att- <i>rev</i>	Lin	8.82×10^{-1} (1.45×10^{-1})	6.76×10^{-1} (1.15×10^{-1})	1.44×10^{-2} (3.47×10^{-4})	2.44×10^{-3} (2.34×10^{-4})	0 [#]	0.997	0.842	1.00	43.2	88
2S4R-att- <i>rev</i>	Log	$5.13 \times 10^{+2}$ ($5.29 \times 10^{+2}$)	$3.94 \times 10^{+2}$ ($2.02 \times 10^{+2}$)	6.22×10^{-3} (2.80×10^{-4})	6.95×10^{-3} (2.86×10^{-4})	0 [#]	0.930	0.997	21.6	0.84	98
3S5R-att- <i>irrev</i>	Lin	$3.05 \times 10^{+0}$ ($2.14 \times 10^{+0}$)	$2.53 \times 10^{+0}$ ($1.80 \times 10^{+0}$)	1.17×10^{-2} (6.18×10^{-4})	1.41×10^{-2} (1.46×10^{-3})	7.68×10^{-3} (3.82×10^{-4})	0.998	0.867	0.61	36.4	83

The eluted mass fraction in the experiment was 82.7%.

Standard errors are given in parenthesis. [†]Denotes whether the models was fitted to the non-transformed (lin) or log₁₀-transformed concentration data (log); [‡]modelling efficiency according to [Loague and Green \(1991\)](#) calculated for non-transformed data: $EF = (\sum (O_i - O_{mean})^2 - \sum (O_i - P_i)^2) / \sum (O_i - O_{mean})^2$, where O_i and P_i are the observed and predicted values, respectively and O_{mean} is the arithmetic mean of the observed values; [§]modelling efficiency calculated on the basis of the log₁₀-transformed data; [¶]sum of squares calculated on the basis of the non-transformed data; ^{††}sum of squares calculated on the basis of the log₁₀-transformed data; ^{‡‡}eluted mass fraction; [#]fixed parameters.

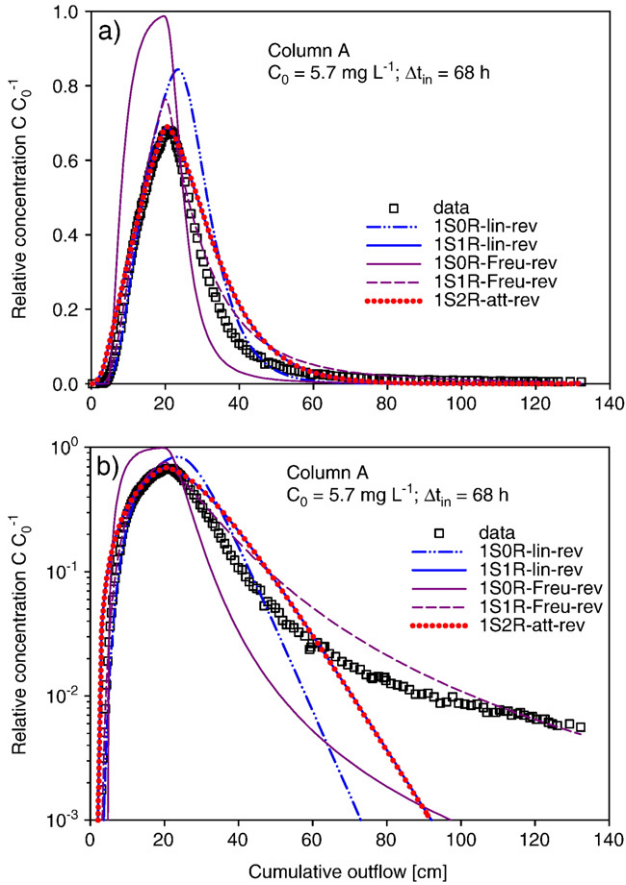


Fig. 5. Normal (a) and semi-log (b) plots of the BTC for column A and different fits of the one-site models. The models with Freundlich sorption were fitted to the \log_{10} -transformed data.

4.2. Transport of SDZ — experimental results

The peak maxima of different treatments were delayed relative to chloride by a factor of 2 to 5 (Fig. 3), which is an arbitrary measure for residence time. The decreasing limb of each BTC is characterized by an extended tailing that exhibits a rather constant slope after about 60 cm of cumulative outflow in the semi-log plot (Fig. 3b). Within the experimental duration of approximately three weeks, a complete breakthrough of SDZ was not achieved due to the pronounced tailing. The BTCs differed in the maximum concentrations as well as the eluted mass fractions. Despite the comparable amount of cumulative irrigation in all experiments, the eluted mass fraction was considerably higher for the experiments with the long pulse application A and B (83 and 61%, respectively) as compared with the short pulse application (experiment C), where only 18% was leached (Table 5).

Concentration profiles of SDZ for the columns with the long pulse application (A, B) showed the highest concentrations at the top of the column, with concentrations steadily decreasing towards the bottom (Fig. 4). In the column with the short pulse application (C) solute concentrations were relatively uniformly distributed. Concentrations were slightly higher

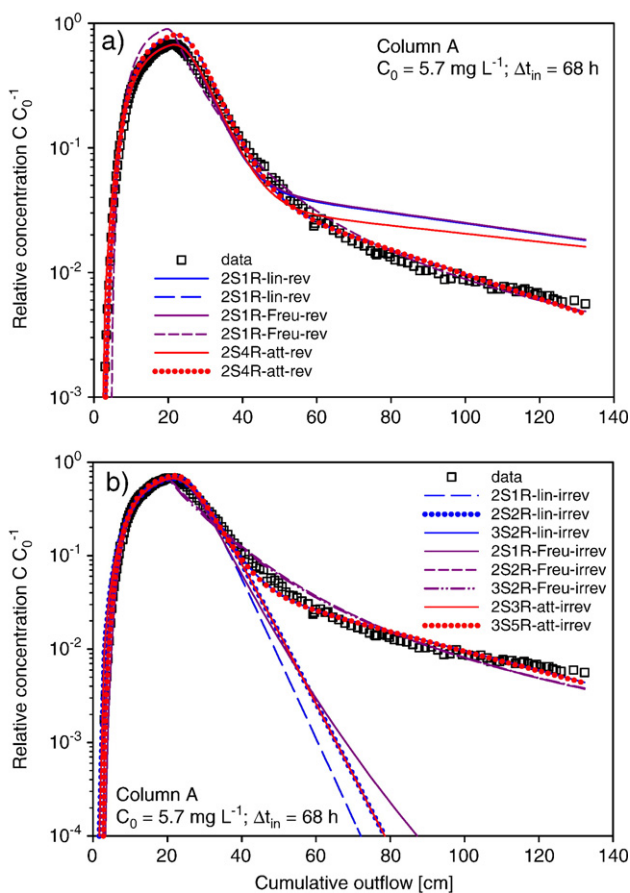


Fig. 6. Semi-log plot of the BTC of column A and different model fits with a) two-site reversible and b) two- or three-site irreversible sorption models. For each model in Fig. 6a both fits to the non-transformed (solid lines) and to the \log_{10} -transformed (dashed or dotted lines) are given. In Fig. 6b the 2S1R-lin-irrev, 2S2R-lin-irrev, 2S1R-Freu-irrev, 2S3R-att-irrev models were fitted to the non-transformed data, the other four models to the \log_{10} -transformed data.

between 2 and 6 cm depth of the column. The difference between the applied and the recovered mass was less than 3% of the applied mass for all experiments (Table 5).

4.3. Transport of SDZ — modelling results

The breakthrough curves of SDZ were fitted using *HYDRUS-1D* assuming different solute–soil–water interaction concepts. The various transport models and their corresponding fits are discussed below in detail for column A. The model complexity was increased from one-site equilibrium models to more complex multiple-site models with reversible or irreversible sorption. The fitted parameters and further details are given in Table 6.

4.3.1. One-site sorption models

Fig. 5 shows the fit of the various one-site models in normal and semi-log representation. In general all one-site sorption models overestimated the leaching of SDZ. They could not

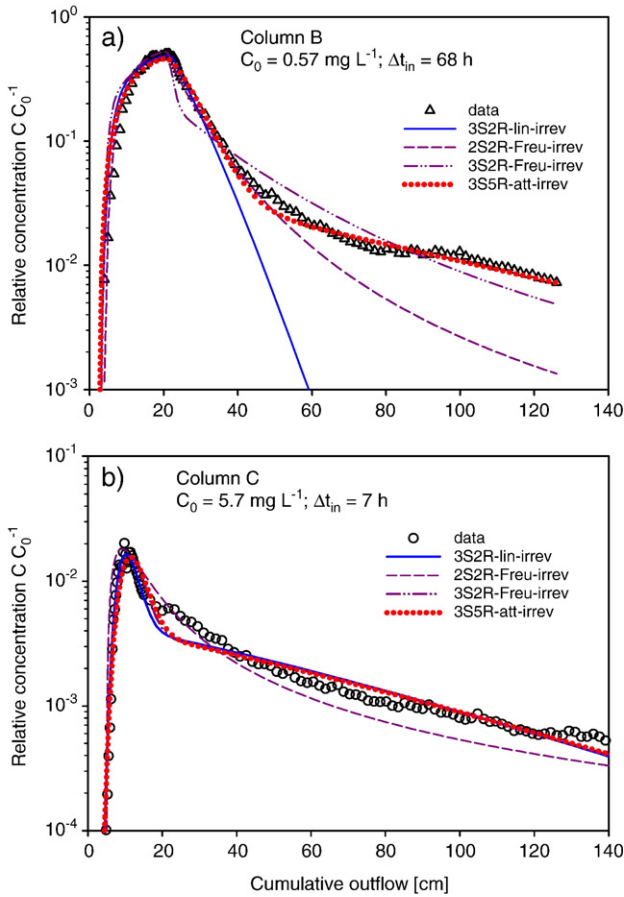


Fig. 7. Semi-log plot of the BTC of column B (a) and C (b) and different fits of two- or three-site irreversible models. For column B (a) the 3S2R-lin-irrev and the 3S5R-att-irrev models were fitted to the \log_{10} -transformed data, while the other two models to the non-transformed data. For column C (b) all models were fitted to the \log_{10} -transformed data.

account for the mass remaining in the soil column at the end of the experiment (Table 6). Notice that if sorption was assumed to be rate-limited and reversible, the predicted curves with the linear sorption (1S1R-lin-rev) and the kinetic attachment/detachment model (1S2R-att-rev) are almost identical since the models are mathematically equivalent. Only the curve fitted with the Freundlich rate-limited reversible sorption (1S1R-Freu-rev) described approximately the main features of the observed BTC. Although the maximum peak concentration and the decreasing limb were only slightly overestimated the difference in the mass balance was still relatively large (14%, Table 6). Both models involving Freundlich sorption isotherms were fitted to the \log_{10} -transformed data, which gives more weight to the lower concentrations in the tailing. More weight is placed on the peak concentrations in the non-transformed data. Each model was fitted to the non-transformed and the \log_{10} -transformed concentration data. To select one fit for presentation, we focused on the ability of the model to match the tailing. This rather subjective choice is not always supported by the modelling efficiency or the sum of squares. Because the models involving kinetic sorption matched the observations better, but

Table 7
Fitting parameters of the different isotherm-based (upper part) and attachment/detachment (lower part) models for column B

Model	Fit [†]	K_f ($\text{kg}^{-1}\text{L}^{3m} \text{mg}^{1-m}$)	m	α_2 (h^{-1})	f	β_3 (h^{-1})	EF [‡]	EF _{log} [§]	SSQ [¶]	SSQ _{log} ^{††}	EM ^{**} (%)
Linear sorption model											
3S2R-lin-irrev	Lin	6.49×10^{-1} (2.72×10^{-2})	1 [#]	7.53×10^{-2} (1.13×10^{-2})	2.46×10^{-1} (5.18×10^{-2})	3.29×10^{-2} (8.52×10^{-4})	0.988	-9.89	0.016	828	59
Freundlich sorption models											
2S2R-Freu-irrev	Lin	4.61×10^{-1} (1.02×10^{-2})	4.98×10^{-1} (5.47×10^{-2})	7.80×10^{-2} (2.42×10^{-3})	0 [#]	2.80×10^{-2} (4.19×10^{-4})	0.993	-0.687	0.009	128	56
3S2R-Freu-irrev	Log	6.08×10^{-1} (2.14×10^{-1})	4.54×10^{-1} (1.40×10^{-1})	2.76×10^{-2} (7.92×10^{-3})	2.10×10^{-3} (1.62×10^{-2})	2.53×10^{-2} (1.18×10^{-4})	0.931	0.264	0.096	55.9	59
Model	Fit [†]	β_1 (h^{-1})	γ_1 (h^{-1})	β_2 (h^{-1})	γ_2 (h^{-1})	β_3 (h^{-1})	EF [‡]	EF _{log} [§]	SSQ [¶]	SSQ _{log} ^{††}	EM ^{**} (%)
Attachment/detachment model											
3S5R-att-irrev	Log	1.37×10^{-1} (5.75×10^{-2})	1.10×10^{-1} (5.16×10^{-2})	1.29×10^{-2} (3.16×10^{-3})	4.66×10^{-3} (2.27×10^{-3})	2.49×10^{-2} (6.97×10^{-3})	0.981	0.686	0.026	23.8	59

The eluted mass fraction in the experiment was 60.7%.

Standard errors are given in parenthesis. [†]Denotes whether the model was fitted to the non-transformed (lin) or log₁₀-transformed concentration data (log); [‡]modelling efficiency according to [Loague and Green \(1991\)](#) calculated for non-transformed data: $EF = (\sum(O_i - O_{\text{mean}})^2 - \sum(O_i - P_i)^2) / \sum(O_i - O_{\text{mean}})^2$, where O_i and P_i are observed and predicted values, respectively and O_{mean} is the arithmetic mean of the observed values; [§]modelling efficiency calculated on the basis of the log₁₀-transformed data; [¶]sum of squares calculated on the basis of the non-transformed data; ^{††}Sum of squares calculated on the basis of the log₁₀-transformed data; ^{**}eluted mass fraction; [#]fixed parameters.

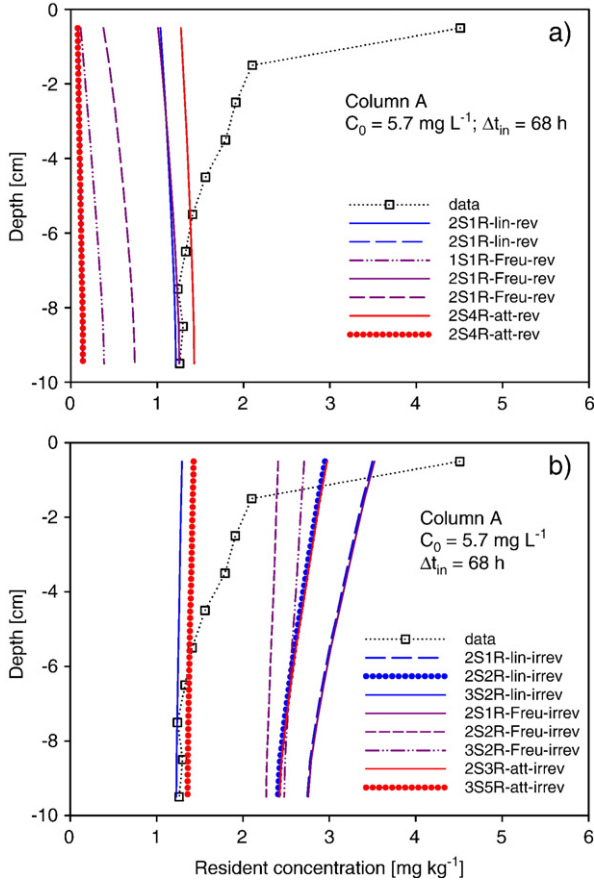


Fig. 8. Measured and modelled soil profiles of resident ^{14}C concentrations in column A. The reversible models are given in Fig. 8a, the irreversible models in Fig. 8b.

still not sufficiently, model complexity should be enhanced to reflect all observed features of the BTC. Therefore, an additional site with kinetic reversible sorption was included in the following models.

4.3.2. Two-site reversible sorption models

The curves fitted to both, the \log_{10} - and non-transformed data using the two-site reversible sorption models are plotted in Fig. 6a. Only the semi-log plot is given because the description of the tailing is especially interesting. The performance of all models was rather similar. The models fitted to the non-transformed data matched well the peak, but overestimated the tailing, whereas the models fitted to the \log_{10} -transformed data overestimated the peak concentrations, but described the tailing well. Despite the mismatch in the tailing of the models fitted to the non-transformed data, EF is larger than for the models fitted to the \log_{10} -transformed data. Whereas $\text{EF}_{10\text{g}}$ is always smaller than EF for the models fitted to the non-transformed data, $\text{EF}_{10\text{g}}$ is larger or only slightly smaller than EF for the models fitted to the \log_{10} -transformed data (Table 6). Since the loss in modelling efficiency ($\text{EF} - \text{EF}_{10\text{g}}$) is smaller for the models fitted to the \log_{10} -transformed data, these fits were preferred. Similarly as for the one-site models, the linear sorption

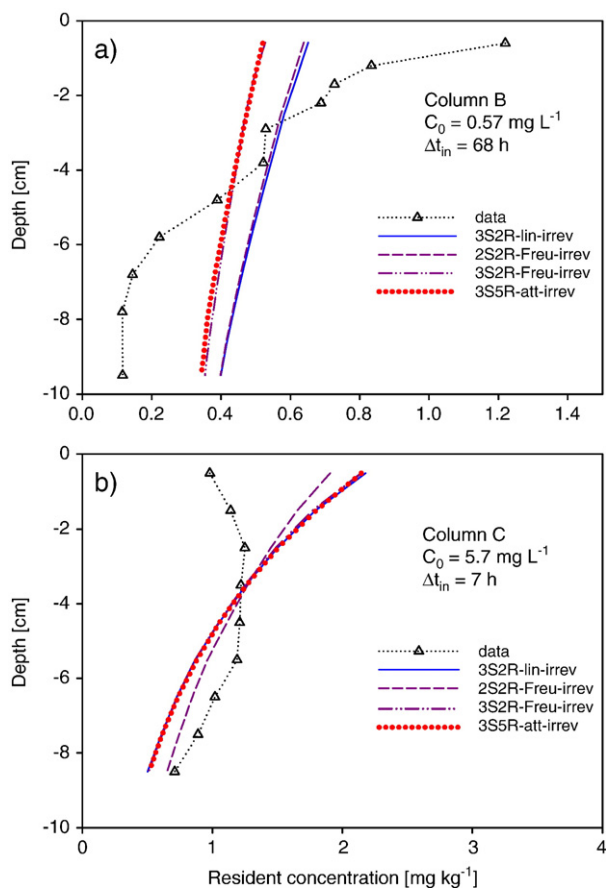


Fig. 9. Measured and modelled soil profiles of resident ^{14}C concentrations in column B (a) and C (b).

model 2S1R-lin-irrev and the attachment/detachment model 2S4R-att-irrev provided almost identical fits. This indicates that the attachment/detachment rates on one fraction of sorption sites are fast compared to the transport velocity and can thus be approximated by instantaneous sorption. However, the leached mass fraction was still overestimated in all two-site rate-limited reversible sorption models. At least one process is, thus missing that can account for the solute mass remaining in the soil column. While sorption is often assumed to be a reversible process, desorption kinetics may be very slow compared to the duration of the experiment and sorption may then appear to be irreversible. Whether irreversible sorption processes can account for the mass remaining in the soil column and describe the observed BTC was tested with the following models that consider irreversible sorption.

4.3.3. Two- or three-site irreversible sorption models

The curves fitted with models considering two or three sorption sites with one site being irreversible are presented in Fig. 6b. The optimized parameters are given in Table 6. The peak concentrations were well described by all irreversible models. However, all two-site models except the 2S2R-Freu-irrev model failed to predict the extended tailing (Fig. 6b) and underestimated the leached mass fraction (Table 6). The simulated curves of the 2S2R-lin-irrev

Table 8
Fitting parameters of the different isotherm-based (upper part) and attachment/detachment (lower part) models for column C

Model	Fit [†]	K_f ($\text{kg}^{-1} \text{L}^{3m} \text{mg}^{1-m}$)	m	α_2 (h^{-1})	f	β_3 (h^{-1})	EF [‡]	EF _{log} [§]	SSQ [¶]	SSQ _{log} ^{††}	EM ^{‡‡} (%)
Linear sorption model											
3S2R-lin-irrev	Lin	$6.15 \times 10^{+0}$ (8.16×10^{-1})	1 [#]	9.41×10^{-3} (2.05×10^{-3})	1.65×10^{-1} (2.32×10^{-2})	1.06×10^{-1} (7.23×10^{-3})	0.968	0.526	0.003	24.3	17
Freundlich sorption models											
2S2R-Freu-irrev	Log	8.59×10^{-1} (4.55×10^{-4})	2.03×10^{-1} (1.58×10^{-4})	1.99×10^{-1} (1.19×10^{-4})	0 [#]	8.63×10^{-2} (1.54×10^{-4})	0.753	0.760	0.023	12.3	19
3S2R-Freu-irrev	Log	$7.07 \times 10^{+0}$ ($1.20 \times 10^{+0}$)	$1.06 \times 10^{+0}$ (4.00×10^{-2})	8.22×10^{-3} (1.90×10^{-3})	1.74×10^{-1} (2.72×10^{-2})	1.06×10^{-1} (7.39×10^{-3})	0.927	0.544	0.007	23.3	17
Model	Fit [†]	β_1 (h^{-1})	γ_1 (h^{-1})	β_2 (h^{-1})	γ_2 (h^{-1})	β_3 (h^{-1})	EF [‡]	EF _{log} [§]	SSQ [¶]	SSQ _{log} ^{††}	EM ^{‡‡} (%)
Attachment/detachment model											
3S5R-att-irrev	Log	$5.91 \times 10^{+0}$ ($3.54 \times 10^{+0}$)	$2.81 \times 10^{+0}$ ($1.95 \times 10^{+0}$)	7.45×10^{-2} (1.55×10^{-2})	8.51×10^{-3} (1.99×10^{-3})	1.05×10^{-1} (7.46×10^{-3})	0.918	0.544	0.007	23.3	18

The eluted mass fraction in the experiment was 17.8%.

Standard errors are given in parenthesis. [†]Denotes whether the model was fitted to the non-transformed (lin) or log₁₀-transformed concentration data (log); [‡]modelling efficiency according to Loague and Green (1991) calculated for non-transformed data: $EF = (\sum(O_i - O_{\text{mean}})^2 - \sum(O_i - P_i)^2) / \sum(O_i - O_{\text{mean}})^2$, where O_i and P_i are the observed and predicted values, respectively and O_{mean} is the arithmetic mean of the observed values; [§]modelling efficiency calculated on the basis of the log₁₀-transformed data; [¶]sum of squares calculated on the basis of the non-transformed data; ^{††}sum of squares calculated on the basis of the log₁₀-transformed data; ^{‡‡}eluted mass fraction; [#]fixed parameters.

and the 2S3R-att-irrev model were identical, as expected. In case of the Freundlich sorption (2S2R-Freu-irrev), the observed and predicted BTCs were in close agreement, apart from a slight underestimation of concentrations in the beginning of the decreasing limb. The calculated eluted mass fraction (80%) was close to the observed fraction, too. An additional instantaneous sorption site (3S2R-Freu-irrev) did not further improve the model performance.

The additional sorption site in the three-site model with linear sorption (3S2R-lin-irrev) and the attachment/detachment model (3S5R-att-irrev) resulted in a very good fit of the tailing and only a slight overestimation of the peak concentrations. Both predicted curves were nearly identical with a leached mass fraction of about 88%. In general, the long tailing characterized by two distinct slopes of the measured BTC required a model that either considered two sorption sites with kinetic desorption, such as 3S2R-lin-irrev or 3S5R-att-irrev, or one kinetic desorption site combined with non-linear sorption/desorption, such as 2S2R-Freu-irrev or 3S2R-Freu-irrev. The large standard errors of the estimated parameters (Table 6) should, however, be recognized as a hint for overparameterization of the used models.

In terms of EF and SSQ, the 3S5R-att-irrev model performed slightly better than models with three-site isotherm-based irreversible sorption and the 2S2R-Freu-irrev model. Note that in contrast to the other two models, the 3S5R-att-irrev model was fitted to the non-transformed data. The comparability of EF and SSQ (EF_{\log} and SSQ_{\log}) is therefore limited. But from only one measured BTC it cannot be decided whether (i) sorption is linear or non-linear, nor (ii) if two or three kinetic sorption sites are required, nor (iii) whether the fast sorption process can be approximated by instantaneous sorption. Therefore, the ability of the four models, which performed best for experiment A, was tested to describe the two BTCs measured under different application protocols.

4.3.4. Model description for different application protocols

Model fits and their parameters for experiment B are given in Fig. 7a and Table 7, respectively. The 2S2R-Freu-irrev model described the peak of the BTC well, but underestimated the tailing and, thus, the eluted mass fraction. Out of the three-site models only the 3S5R-att-irrev model matched the observed BTC as well as the eluted mass fraction (52%). The other three-site models either failed to describe the shape of the peak (3S2R-Freu-irrev) or the tailing (3S2R-lin-irrev). Since the 3S5R-att-irrev differs from the 3S2R-lin-irrev model, attachment/detachment rates on the fast kinetic sites was too slow to be approximated by instantaneous sorption.

The simulated BTCs for experiment C with the short application pulse are plotted in Fig. 7b. The three-site models are nearly identical, and all curves roughly described the observed BTC. The highest peak concentration and concentrations in the beginning of the tailing (between 20 and 40 cm of cumulative outflow) were underestimated. The 2S2R-Freu-irrev model predicted the latter part better, but underestimated the concentrations in the tailing. As was observed for experiment A with the same input concentration, the fast attachment/detachment process in the 3S5R-att-irrev model could be approximated by instantaneous sorption (3S2R-lin-irrev). Because the fitted Freundlich exponent was close to 1, the simulated curve with the 3S2R-Freu-irrev model was almost identical to the latter two models.

Thus, only the 3S5R-att-irrev model was flexible enough to predict the observed BTCs of all three experiments. Note that the standard errors of the five estimated rate parameters are relatively large. Hence, the accuracy of the estimates is reduced, which might be a result of the high flexibility of the model. As already known in soil physics the results demonstrate that experiments with different boundary conditions are necessary to identify the relevant sorption processes. Although it is highly unlikely that, because of the complexity of the sorption processes, the

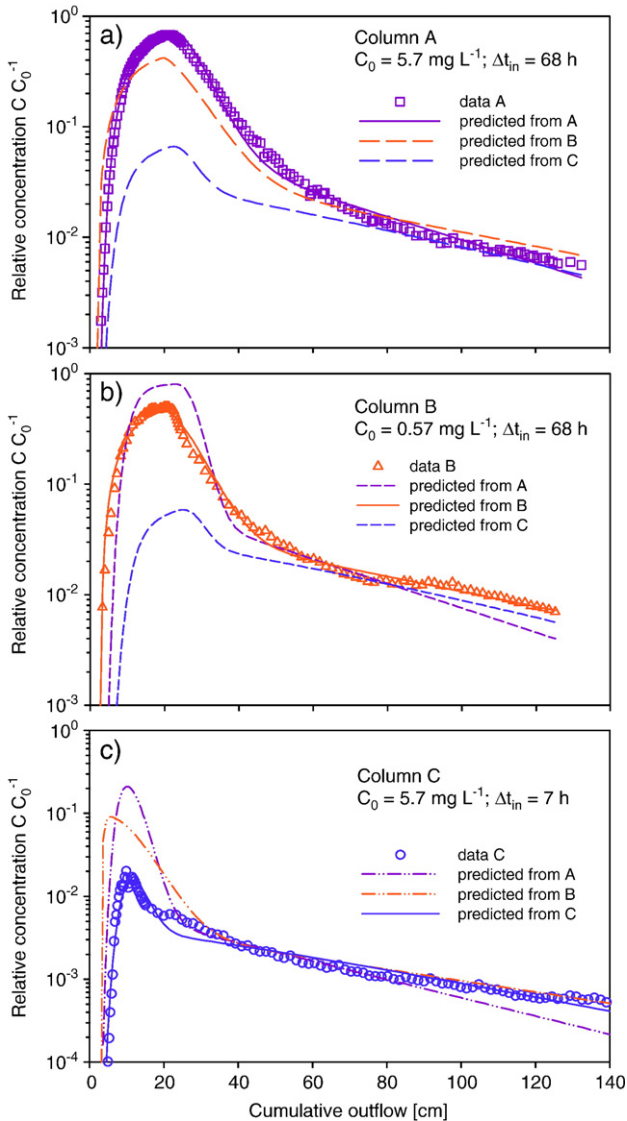


Fig. 10. Measured, fitted and predicted BTCs with the 3S5R-att-irrev model for experimental conditions A (a), B (b) and C (c).

calibrated parameters represent unique solutions of the inverse problem, they did provide a very good description of the measured BTCs. However, the optimal parameter sets differed widely between the three experiments. Variation of other boundary conditions, such as irrigation rate, might help to further elucidate possible sorption processes.

4.3.5. Concentration profiles

Simulated concentration profiles for the different sorption models are given in Figs. 8 and 9. None of the simulated profiles matched the measurements, despite good fits for the BTCs.

Including observed concentration profile data in the numerical inversion of models with irreversible sorption did not result in a parameter set that could considerably better simulate the measured soil concentration profiles (data not shown).

A first-order irreversible sorption process results in an exponential decrease in the soil resident concentration profile. However, no parameter combination was found for experiments A and B to match all features of the profile concentrations under the prevailing boundary conditions, i.e. the high concentrations in the upper part followed by the steep concentration gradient and the constant concentration level in the lower part of the column. Still, only models involving irreversible sorption processes were able to predict higher resident concentrations at the top than at the bottom of the column (Fig. 8a and b) after long leaching periods.

In experiment C a more uniform soil concentration distribution was observed (Fig. 9b). To account for the large mass fraction remaining in the column, the fitted irreversible sorption rate was larger in all models than for experiments A or B. However, the modelled soil concentration gradient was steepest for this set of parameters, and did not match the observed shape.

4.3.6. Parameter comparison and predictability

Although the 3S5R-att-irrev model might not be the adequate process description, the optimized parameter values for the different experiments (Tables 6, 7 and 8) showed some trends. The comparability of the parameter sets is justified by the fact that soil to solution ratios are similar in all columns. Since most mass was retained in the soil in experiment C parameter β_3 and sorption affinity were both the highest for this experiment. The attachment rate coefficient towards the irreversible sorption site β_3 irreversibly removes solute mass from the transport domain. Sorption affinity reduces the solute transport velocity compared to the water flow and can be estimated from the ratio between the attachment and the detachment rate coefficients (β_i/γ_i). The slow reversible attachment/detachment rate coefficients were within the same range, whereas the rate coefficients for the fast sorption site differed by three orders of magnitude, with the largest values for experiment A and smallest for experiment B.

However, if the 3S5R-att-irrev model included all relevant processes occurring during the experiments and if its parameters were constant (i.e. concentration independent), the optimal parameters for all experimental conditions should be identical. The predictive power of the 3S5R-att-irrev model was tested to describe the BTCs. The optimal parameter set for one experiment was used to predict the BTC for the other two application scenarios (Fig. 10). The earliest breakthrough was always predicted using the parameters of experiment B, the latest using the parameters of experiment C. The observed peak concentrations and the eluted mass fractions were never met by the forward calculations, because the values of β_3 were too different. However, the tailing is described well by all parameter combinations (Fig. 10). The tailing of the BTC cannot proceed faster than $\exp(-\alpha_{\text{slow}}t)$, suggesting that it drops with $\exp(-\beta t)$, where $\beta = \alpha_{\text{slow}} - \delta$ with $\delta > 0$ (Vereecken et al., 1999). Here β is the slope of the tailing in the semi-log plot for two-site kinetic sorption models (equivalent to the 2S2R-lin-rev or 2S4R-att-rev models) and α_{slow} is the smallest sorption rate coefficient. For the 3S5R-att-irrev model the determining rate coefficient for the tailing is the smallest desorption rate γ_2 , because the irreversible sorption process does not influence the slope of the tailing. For all sets of parameters, the values of γ_2 are in the same order and thus the slopes of the tailing are expected to be similar, too. Due to the differences in the fitted 3S5R-att-irrev model parameters for the three experiments, we did not expect to find a set of parameters that fits all experiments equally well by simultaneous fitting. We thus, did not add an

option for simultaneous fitting of multiple experiments to the applied version of the *HYDRUS-1D* model.

5. Discussion

Incomplete breakthrough of sulfonamides has previously been reported during transport of SDZ (Kreuzig and Hölte, 2005), sulfachloropyridazine (Boxall et al., 2002; Kay et al., 2005b) and sulfamethoxazole (Drillia et al., 2005). However, the effect of different boundary conditions regarding the solute application on the transport was not yet investigated. Kreuzig and Hölte (2005) found only 4% of the applied SDZ in the leachate compared to 43% of a simultaneously applied conservative tracer. They also found more than 60% of the applied ^{14}C -labelled SDZ as non-extractable residues in the upper 5 cm of the column after 6 days of irrigation. The resulting concentration profile is in accordance with our studies, although detailed information about the BTCs was lacking. Low recoveries were shown for SDZ by Kreuzig et al. (2003) or Hamscher et al. (2005), especially for aged soil residues. Because of the lack of proved degradation products, the missing mass may as well be non-extractable, apparently irreversibly sorbed parent substance. The model concept proposed to describe the transport of sulfamethoxazole included non-linear Freundlich sorption as well as a rate-limited mass transfer between the flowing bulk liquid phase and a stagnant water film attached to the soil particles (Drillia et al., 2005). However, for soils with little organic material, a strong sorption hysteresis was also observed, which might be described by a second, slower reversible or even an irreversible sorption process (Drillia et al., 2005). Due to its two ionizable functional groups, the charge of SDZ depends on the prevailing pH-value. Although the pH-dependent species of SDZ exhibit different sorption properties (e.g. Gao and Pedersen, 2005), the proposed model concepts did not account for pH-speciation. This is justified because pH did not change during the experiments. Thus, the ratio of the dominant species was assumed to be constant. Because the neutral and the anionic species were dominant in the column experiments, cation exchange as one of the sorption processes may be negligible. Anion sorption of SDZ on positively charged iron oxides might be anticipated. In independent batch sorption experiments sorption of ^{14}C -sulfadiazine was determined to be non-linear and rate-limited, whereas desorption is very slow or even irreversible (data not shown). As already reported by Tolls (2001) for various pharmaceuticals, common sorption concepts (K_{OC} , linear equilibrium isotherms) are inappropriate for the description of these experiments. This rather complex sorption behavior will be addressed in a forthcoming article.

Although process-oriented transport studies for veterinary pharmaceuticals are still rare, comparable experimental protocols are commonly used for the estimation of the transport parameters for other environmental pollutants, such as pesticides or bacteria. Prata et al. (2003) described the BTC of the herbicide atrazine in repacked soil columns well with the 3S2R-lin-irrev model. The irreversible sorption process accounted for 40 to 50% of the applied mass remaining in the soil column after the leaching period, while even the concentration profile was relatively well reproduced. A similar long tailing due to chemical non-equilibrium sorption was observed for the hormone testosterone in repacked soil columns (Casey et al., 2004). They successfully described the observed BTCs with a one-site kinetic Freundlich sorption model, having a first-order degradation in the solid phase. The attachment/detachment concept gave the best predictions for all experiments. This approach is commonly used to describe the transport of small particles such as bacteria or viruses in soils or aquifers (Schijven and Hassanizadeh, 2000). In these studies the characteristic soil concentration profiles and the extended tailing are often observed (Schijven et al., 2002; Bradford et al., 2002, 2003). However, in particle transport

studies additional processes, such as blocking, filtration or straining are included to describe how the size of the particles and their surface properties affect the transport behavior. The required parameters can even be determined independently (Bradford et al., 2002, 2003). These authors considered, for example, blocking as depth-dependent. This concept results in high resident concentrations near the source of the particle release, i.e. the top of the column with very steep concentration gradients.

However, a depth-dependent process, which might better describe the observed soil concentration profiles in this study, cannot be justified for a solute such as SDZ. Nevertheless, the poor model performance for the concentration profiles is a hint that at least one process is lacking in the model. Since our chemical analysis of SDZ was restricted to ^{14}C only, we have no information available on possible transformation reactions of the ^{14}C -labelled parent compound and its daughter products in the leachate or the soil. Transformation might affect the overall transport in the following manner: It is anticipated that transformation products exhibit different sorption properties (isotherm, kinetics, reversibility) as compared to the parent compound. In contrast to the parent compound which is applied on top of the soil column, the transformation products are formed during the course of the experiment within the soil column. The concentration of the parent compound consequently decreases. The concentrations of the transformation products may increase or decrease according to their sorption properties and their successive transformation. The simultaneously occurring sorption and transformation processes that may depend on time and concentration, result in different BTCs and soil concentration profiles than predicted with the presented effective models for ^{14}C -SDZ. An estimation of the effect of the occurrence of transformation products during the experiments would be highly speculative, since only the superimposed BTCs and soil concentration profiles of the parent and possible transformation products were determined by ^{14}C -analysis. Additionally there is too little information in the literature on the identity, concentration, transformation pathways, transformation kinetics and sorption properties of the transformation products. To our knowledge no information exists on the fate of acetyl-SDZ and hydroxy-SDZ, two of the known transformation products of SDZ, in soils.

6. Conclusions

The transport of SDZ depends on the application protocol of the solute, i.e. the input concentration and the pulse duration. The observation of low concentrations in the tailing and the determination of soil resident concentrations was only possible due to the ^{14}C -analysis. The observed differences in peak concentrations and eluted mass fraction are caused by time- and concentration-dependent sorption processes. Only the complex three-site kinetic sorption model with two reversible and one irreversible sorption site was flexible enough to describe the complete observed BTCs for the various application scenarios. Despite the good agreement for the BTCs, the observed and modelled concentration profiles in the soil differed substantially. Therefore, common approaches for process identification on the basis of the main peak breakthrough without the observation of the tailing and the concentration profile are precarious. Reasons for the discrepancy between observations and model predictions might be: (i) possible transformation reactions, which were out of the scope of the experimental and model investigations, (ii) inappropriate mathematical concepts for the sorption processes, i.e. isotherms and rate-laws and (iii) the assumption of sorption irreversibility. Although SDZ reaches the soil environment typically as ingredient of manure, the results imply that leaching of SDZ might be enhanced if applied in higher concentrations on soils near water saturation shortly before the next rain event.

References

- Berger, K., Petersen, B., Pfaue, H.B., 1986. Persistenz von Gülle-Arzneistoffen in der Nahrungskette. *Archiv für Lebensmittelchemie* 37, 99–102.
- Boxall, A.B.A., Blackwell, P., Cavallo, R., Kay, P., Tolls, J., 2002. The sorption and transport of a sulfonamide antibiotic in soil systems. *Toxicology Letters* 131, 19–28.
- Boxall, A.B.A., Fogg, L.A., Blackwell, P.A., Kay, P., Pemberton, E.J., Croxford, A., 2004. Veterinary medicines in the environment. *Reviews of Environmental Contamination and Toxicology* 180, 1–91.
- Bradford, S.A., Yates, S., Betthar, M., Simunek, J., 2002. Physical factors affecting the transport and fate of colloids in saturated porous media. *Water Resources Research* 38, doi:10.1029/2002WR001340.
- Bradford, S.A., Simunek, J., Betthar, M., van Genuchten, M.T., Yates, S., 2003. Modeling colloid attachment, straining, and exclusion in saturated porous media. *Environmental Science and Technology* 37, 2242–2250.
- Burkhardt, M., Stamm, C., Waul, C., Singer, H., Müller, S., 2005. Surface runoff and transport of sulfonamide antibiotics and tracers on manured grassland. *Journal of Environmental Quality* 34, 1363–1371.
- Casey, F.X.M., Hakk, H., Simunek, J., Larsen, G., 2004. Fate and transport of testosterone in agricultural soils. *Environmental Science and Technology* 38, 2400–2409.
- Christian, T., Schneider, R.J., Färber, H.A., Skutlarek, D., Meyer, M.T., Goldbach, H.E., 2003. Determination of antibiotic residues in manure, soil and surface waters. *Acta Hydrochimica et Hydrobiologica* 31, 36–44.
- Drillia, P., Stamatielou, K., Lyberatos, G., 2005. Fate and mobility of pharmaceuticals in solid matrices. *Chemosphere* 60, 1034–1044.
- Flury, M., 1996. Experimental evidence of transport of pesticides through field soils — a review. *Journal of Environmental Quality* 25, 25–45.
- Fortin, J., Flury, M., Jury, W., Streck, T., 1997. Rate-limited sorption of simazine in saturated soil columns. *Journal of Contaminant Hydrology* 25, 219–234.
- Gao, J., Pedersen, J.A., 2005. Adsorption of sulfonamide antimicrobial agents to clay minerals. *Environmental Science and Technology* 39, 9509–9516.
- Grote, M., Vockel, A., Schwarze, D., Mehlich, A., Freitag, M., 2004. Fate of antibiotics in food chain and environment originating from pig fattening. *Fresenius Environmental Bulletin* 13, 1214–1216.
- Hamscher, G., Pawelzick, H.T., Höper, H., Nau, H., 2005. Different behaviour of tetracyclines and sulfonamides in sandy soils after repeated fertilization with liquid manure. *Environmental Toxicology and Chemistry* 24, 861–868.
- Hillel, D., 1998. *Environmental Soil Physics*. Academic Press, San Diego.
- Höper, H., Kues, J., Nau, H., Hamscher, G., 2002. Eintrag und Verbleib von Tierarzneimittelwirkstoffen in Böden. *Bodenschutz* 4, 141–148.
- Jørgensen, S.E., Halling-Sørensen, B., 2000. Drugs in the environment. *Chemosphere* 40, 691–699.
- Kay, P., Blackwell, P.A., Boxall, A.B., 2004. Fate of veterinary antibiotics in a macroporous tile drained clay soil. *Environmental Toxicology and Chemistry* 23, 1136–1144.
- Kay, P., Blackwell, P.A., Boxall, A.B., 2005a. Transport of veterinary antibiotics in overland flow following the application of slurry to arable land. *Chemosphere* 59, 951–959.
- Kay, P., Blackwell, P.A., Boxall, A.B., 2005b. Column studies to investigate the fate of veterinary antibiotics in clay soils following slurry application to agricultural land. *Chemosphere* 60, 497–507.
- Kreuzig, R., Hölte, S., 2005. Investigations on the fate of sulfadiazine in manured soil: laboratory experiments and test plot studies. *Environmental Toxicology and Chemistry* 24, 771–776.
- Kreuzig, R., Kullmer, C., Matthies, B., Hölte, S., Diekmann, H., 2003. Fate and behavior of pharmaceutical residues in soils. *Fresenius Environmental Bulletin* 12, 550–558.
- Kroker, R., 1983. Aspects of the elimination of antibiotics after treatment of domestic animals. *Wissenschaft und Umwelt* 4, 305–308.
- Loague, K., Green, R.E., 1991. Statistical and graphical methods for evaluating solute transport models: overview and application. *Journal of Contaminant Hydrology* 7, 51–73.
- Pfeifer, T., Tuerk, J., Fuchs, R., 2005. Structural characterization of sulfadiazine metabolites using H/D exchange combined with various MS/MS experiments. *Journal of the American Society for Mass Spectrometry* 16, 1687–1694.
- Pignatello, J.J., Xing, B., 1996. Mechanisms of slow sorption of organic chemicals to natural particles. *Environmental Science and Technology* 30, 1–11.
- Prata, F., Lavorenti, A., Vanderborght, J., Burael, P., Vereecken, H., 2003. Miscible displacement, sorption and desorption of atrazine in a Brazilian Oxisol. *Vadose Zone Journal* 2, 728–738.
- Sacher, F., Lange, F.T., Brauch, H.-J., Blankenhorn, I., 2001. Pharmaceuticals in groundwaters — analytical methods and results of a monitoring program in Baden-Württemberg, Germany. *Journal of Chromatography, A* 938, 199–210.

- Schijven, J.F., Hassanizadeh, S.M., 2000. Removal of viruses by soil passage: overview of modeling, processes, and parameters. *Critical Review in Environmental Science and Technology* 30, 49–127.
- Schijven, J.F., Šimuňek, J., 2002. Kinetic modeling of virus transport at the field scale. *Journal of Contaminant Hydrology* 55, 113–135.
- Schijven, J.F., Hassanizadeh, S.M., de Bruin, H., 2002. Two-site kinetic modeling of bacteriophages transport through columns of saturated dune sand. *Journal of Contaminant Hydrology* 57, 259–279.
- Simunek, J., Šejna, M., van Genuchten, M.T., 1998. The HYDRUS-1D software package for simulating the one-dimensional movement of water, heat, and multiple solutes in variably saturated media. Version 2.0. ICGWMC-TPS-70, International Ground Water Modeling Center, Colorado School of Mines, Golden, Colorado, p. 202.
- Streck, T., Poletika, N.N., Jury, W.A., Farmer, W.W., 1995. Description of simazine transport with rate-limited, two-stage, linear and nonlinear sorption. *Water Resources Research* 31, 811–822.
- Thiele-Bruhn, S., 2003. Pharmaceutical antibiotic compounds in soil — a review. *Journal of Plant Nutrition and Soil Science* 166, 145–167.
- Thiele-Bruhn, S., Aust, M.-O., 2003. Effects of pig slurry on the sorption of sulfonamide antibiotics in soil. *Archives of Environmental Contamination and Toxicology* 47, 31–39.
- Tolls, J., 2001. Sorption of veterinary pharmaceuticals in soils: a review. *Environmental Science and Technology* 35, 3397–3406.
- Toride, N., Leij, F.J., van Genuchten, M.T., 1999. The CXTFIT code for estimating transport parameters from laboratory or field tracer experiments. Version 2.1. US Salinity Laboratory, Agricultural Research Service US Department of Agriculture, Riverside, California, Research Report, vol. 137.
- van Genuchten, M.T., Wagenet, R.J., 1989. Two-site/two-region models for pesticide transport and degradation: theoretical development and analytical solutions. *Soil Science Society of America Journal* 53, 1303–1310.
- van Genuchten, M.T., Wierenga, P.J., 1976. Mass transfer studies in sorbing porous media: I. analytical solutions. *Soil Science Society of America Journal* 40, 473–481.
- Vereecken, H., Jaeckel, U., Georgescu, A., 1999. Asymptotic analysis of solute transport with linear nonequilibrium sorption in porous media. *Transport in Porous Media* 36, 189–210.